

A new analytical approach for modelling the added mass and hydrodynamic interaction of two cylinders subjected to large motions in a potential stagnant fluid

Romain Lagrange^a, Xavier Delaune^a, Philippe Piteau^a,
Laurent Borsoi^a, José Antunes^b

^a*Den-Service d'études mécaniques et thermiques (SEMT), CEA, Université Paris-Saclay, F-91191, Gif-sur-Yvette, France*

^b*Centro de Ciências e Tecnologias Nucleares, Instituto Superior Técnico, Universidade de Lisboa, Estrada Nacional 10, Km 139.7, 2695-066 Bobadela LRS, Portugal*

Received *****; accepted after revision ++++++

Presented by *****

Abstract

A potential theory is presented for the problem of two moving cylinders, with possibly different radii, large motions, immersed in an perfect stagnant fluid. We show that the fluid force is the superposition of an added mass term, related to the time variations of the potential, and a quadratic term related to its spatial variations. We provide new simple and exact analytical expressions for the fluid added mass coefficients, in which the effect of the confinement is made explicit. The self-added mass (resp. cross-added mass) is shown to decrease (resp. increase) with the separation distance and increase (resp. decreases) with the radius ratio. We then consider the case in which one cylinder translates along the line joining the centers with a constant speed. We show that the two cylinders are repelled from each other, with a force that diverges to infinity at impact. We extend our approach to the case in which one cylinder is imposed a sinusoidal vibration. We show that the force on the stationary cylinder and the vibration displacement have opposite (resp. identical) axial (resp. transverse) directions. For large vibration amplitudes, this force is strongly altered by the nonlinear effects induced by the spatial variations of the potential. The force on the vibrating cylinder is in phase with the imposed displacement and is mainly driven by the added mass term. The results of this paper are of particular interest for engineers who need to grab the essential features associated to the vibration of a solid body in a still fluid.

Key words: Potential flow; Added mass; Fluid force; Cylinders interaction

1 Introduction

The interaction between a fluid and moving bodies is a fundamental problem which finds many applications, for example in turbomachinery [1], fish schooling [2], heat exchangers tube banks [3, 4], vibration of flexible risers [5], biomechanics of plants [6], or energy harvesting [7, 8, 9, 10] from flapping flags [11]... We refer the reader to the book of Païdoussis et. al. [12] for a complete bibliography of important works in this field. A classical approach to understand the fluid dynamics surrounding the bodies is to consider a potential flow model, in which viscous, rotational vortex and wake effects are disregarded. For large Reynolds numbers and outside the boundary layers, the potential flow theory is expected to provide a good approximation of the solution, or some of its related characteristics as the added-mass, see Chen [13]. The very first discussions of potential flows around two circular cylinders are probably due to Hicks [14], who studied the motion of a cylindrical pendulum inside another cylinder filled with fluid. To solve this problem, Hicks considered the potential due to flow singularities distributed over the fluid domain and the cylinder surfaces. The strengths and locations of the singularities were expressed as a set of iterative equations and the potential in an integral form, suitable for numerical computation [15]. Many investigators [16, 17, 18, 19, 20, 21] then tried to clarify and simplify the method of singularities by Hicks to derive a more tractable expression for the fluid potential. Still, this approximate method remains difficult to apply and as the gap between the cylinders becomes small, a high density of singularities is necessary for the solution to converge. More recently, analytical approaches based on complex analysis and conformal mapping methods [22, 23, 24] have overcome this problem and general theories to determine the flow past multiple bodies have been proposed [25, 26, 27]. The two cylinders problem can be solved in this framework, but here we provide a more flexible method which yields new analytical and simplified expressions for the added mass coefficients. We also show that the large motions of the cylinders induce some strong spatial variations of the potential which yield nonlinear inertial effects of the fluid forces.

This paper is organized as follows. Section 2 presents the problem of two parallel circular cylinders immersed in an inviscid fluid and introduces the governing dimensionless numbers. In § 3, we solve the potential flow problem, provide analytical expressions of the added mass terms and determine the fluid force on the cylinders. In § 4 we test our predictions against published

Email address: `romain.g.lagrange@gmail.com` (Romain Lagrange).

results and consider the case of a vibrating cylinder. Finally, some conclusions are drawn in § 5.

2 Definition of the problem

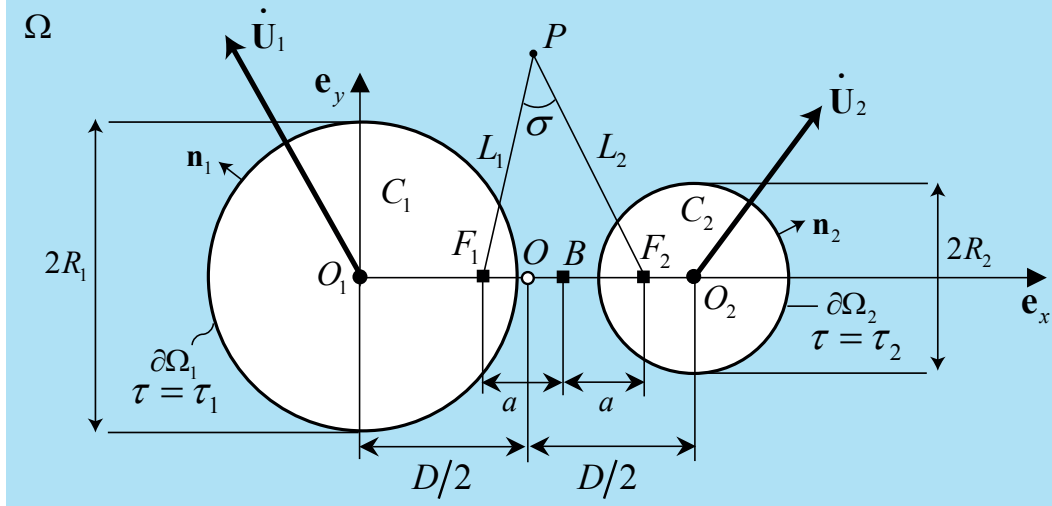


Figure 1. Schematic diagram of the system: two moving cylinders C_i with radii R_i , centers O_i , velocities $\dot{\mathbf{U}}_i(T)$, are immersed in an inviscid fluid Ω . The motions of C_i generate an incompressible and irrotational flow. The instantaneous center-to-center distance is D . The bipolar coordinates $\sigma \in [0, 2\pi[$ and $\tau = \ln(L_1/L_2)$ are used to track the position of a fluid particle P . The points (B, F_1, F_2) are defined in such a way that points lying on the cylinder boundaries $\partial\Omega_i$ have bipolar coordinates $\tau = \tau_i$.

Let C_i , ($i = 1, 2$), be two circular cylinders with radii R_i , immersed in an inviscid fluid of volume mass density ρ . We aim to determine the 2D flow generated by the arbitrary motions of C_i , (Figure 1). For convenience we introduce rescaled quantities to reduce the number of parameters of the problem. We use R_2 to normalize lengths, some characteristic speed V_0 to normalize velocities and ρV_0^2 to normalize pressures. We define

$$r = \frac{R_1}{R_2}, d = \frac{D}{R_2}, \mathbf{u}_i = \frac{\mathbf{U}_i}{R_2}, t = \frac{TV_0}{R_2}, p = \frac{P}{\rho V_0^2}, \mathbf{f}_i = \frac{\mathbf{F}_i}{\rho V_0^2 R_2}, \quad (1)$$

as the radius ratio, the dimensionless center-to-center distance, cylinder displacement, time, fluid pressure and fluid force, respectively. We also introduce the dimensionless separation distance, $\varepsilon = d - (r + 1)$ such that $\varepsilon = 0$ corresponds to cylinders in contact.

3 Theoretical model

3.1 Fluid equations

It is assumed that the fluid is inviscid and the flow generated by the tubes motions is incompressible and irrotational. We thus model the flow with a potential function φ which satisfies the Laplace equation

$$\Delta\varphi = 0 \quad \text{in } \Omega, \quad (2)$$

and the inviscid boundary conditions

$$(\nabla\varphi - \dot{\mathbf{u}}_i) \cdot \mathbf{n}_i = 0 \quad \text{on } \partial\Omega_i. \quad (3)$$

In the above eqs., Ω is the fluid domain and \mathbf{n}_i is the outward normal unit vector to $\partial\Omega_i$ (Figure 1). To account for an unperturbed fluid at infinity we also require that

$$\varphi \rightarrow 0 \quad \text{at infinity.} \quad (4)$$

The fluid pressure p is derived from the unsteady Bernoulli equation

$$p - p_\infty = - \left(\frac{\partial\varphi}{\partial t} + \frac{(\nabla\varphi)^2}{2} \right), \quad (5)$$

where p_∞ is the pressure at infinity. The fluid force on \mathcal{C}_i is obtained by integration of (5) on $\partial\Omega_i$

$$\mathbf{f}_i = \int_{\partial\Omega_i} \left(\frac{\partial\varphi}{\partial t} + \frac{(\nabla\varphi)^2}{2} \right) \mathbf{n}_i ds_i, \quad (6)$$

where ds_i is an infinitesimal element of integration.

The fluid equations must be solved on the instantaneous configuration to account for the possible large displacements of \mathcal{C}_i . This leads us to define a coordinate system based on the kinematics of \mathcal{C}_i and in which the fluid eqs. can be solved analytically.

3.2 Bipolar coordinates

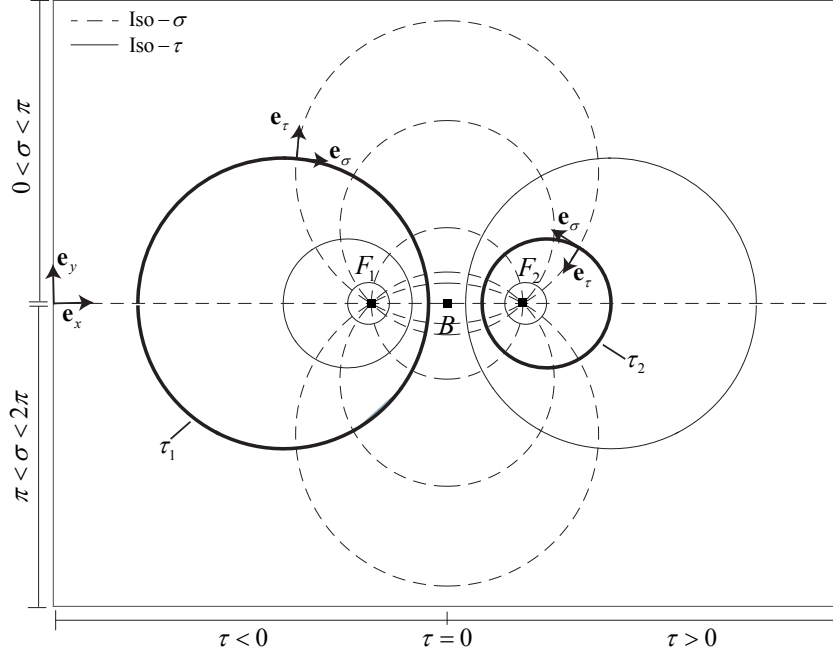


Figure 2. Bipolar coordinate system. The dashed circles are iso-values of σ while the solid circles are iso-values of τ . The two foci points F_i are defined such that $\partial\Omega_i$ has a coordinate τ_i . The points on the x -axis have $\sigma = \pi$ if they lie in between F_1 and F_2 , and $\sigma = 0$ otherwise.

Let (B, F_1, F_2) be three points defined as $\mathbf{OB} = x_B \mathbf{e}_x$ and $\mathbf{BF}_1 = -a \mathbf{e}_x$ and $\mathbf{BF}_2 = a \mathbf{e}_x$, $a > 0$. From these three points, we introduce the bipolar coordinates $\sigma \in [0, 2\pi[$ and $\tau > 0$ to track the position of a fluid particle, as shown in Figure 1. Since the iso- τ contours are circles with centers on the x -axis (Figure 2), one can align $\partial\Omega_i$ with an iso-contour τ_i by setting the position of B and F_i . In Appendix A, we show that

$$x_B = (r^2 - 1) / (2d), \quad (7a)$$

$$a = \sqrt{d^2 - (1+r)^2} \sqrt{d^2 - (1-r)^2} / (2d), \quad (7b)$$

yield iso-contours for the two cylinders

$$\tau_1 = -\sinh^{-1}(a/r) \quad \text{and} \quad \tau_2 = \sinh^{-1}(a). \quad (7c)$$

Introducing $(\mathbf{e}_\sigma, \mathbf{e}_\tau)$ as the coordinate system basis, see Figure 2 and Appendix A, the outward normal unit vector \mathbf{n}_i to $\partial\Omega_i$ is

$$\mathbf{n}_i = (-1)^{i-1} \mathbf{e}_\tau(\sigma, \tau_i), \quad (8)$$

and the infinitesimal measure ds_i of $\partial\Omega_i$ is

$$ds_i = \kappa_{\sigma\tau_i} d\sigma, \quad (9)$$

with $\kappa_{\sigma\tau} = a/(\cosh(\tau) - \cos(\sigma))$.

Finally, the gradient and the Laplace operators in bipolar coordinates are

$$\nabla\phi = \frac{1}{\kappa_{\sigma\tau}} \left(\frac{\partial\phi}{\partial\sigma} \mathbf{e}_\sigma + \frac{\partial\phi}{\partial\tau} \mathbf{e}_\tau \right), \quad (10a)$$

$$\Delta\phi = \left(\frac{1}{\kappa_{\sigma\tau}} \right)^2 \left(\frac{\partial^2\phi}{\partial\sigma^2} + \frac{\partial^2\phi}{\partial\tau^2} \right). \quad (10b)$$

3.3 Solution of the fluid equations

In bipolar coordinates the fluid eqs. (2)-(4) read

$$\frac{\partial^2\varphi}{\partial\sigma^2} + \frac{\partial^2\varphi}{\partial\tau^2} = 0 \quad \text{in } \Omega, \quad (11a)$$

$$\frac{\partial\varphi}{\partial\tau} = g_{ix}\dot{u}_{ix} + g_{iy}\dot{u}_{iy} \quad \text{on } \tau = \tau_i, i = 1, 2, \quad (11b)$$

$$\varphi \rightarrow 0 \quad \text{as } (\sigma, \tau) \rightarrow (0, 0), \quad (11c)$$

with $\dot{u}_{ix}, \dot{u}_{iy}$ the \mathbf{e}_x and \mathbf{e}_y components of $\dot{\mathbf{u}}_i$, respectively. In (11), g_{ix} and g_{iy} are the 2π periodic functions with Fourier components $g_{in} = -2nae^{-n|\tau_i|}$

$$g_{ix}(\sigma) = \kappa_{\sigma\tau_i} \mathbf{e}_x \cdot \mathbf{e}_\tau(\sigma, \tau_i) = -a \frac{\cos(\sigma) \cosh(\tau_i) - 1}{(\cosh(\tau_i) - \cos(\sigma))^2} = \sum_{n=1}^{\infty} g_{in} \cos(n\sigma), \quad (12a)$$

$$g_{iy}(\sigma) = \kappa_{\sigma\tau_i} \mathbf{e}_y \cdot \mathbf{e}_\tau(\sigma, \tau_i) = -a \frac{\sin(\sigma) \sinh(\tau_i)}{(\cosh(\tau_i) - \cos(\sigma))^2} = \sum_{n=1}^{\infty} g_{in} \sin(n\sigma). \quad (12b)$$

The fluid problem being linear in \dot{u}_{ix} and \dot{u}_{iy} , the potential φ is a superposition of two functions φ_x and φ_y , solutions of (11) for $\dot{u}_{iy} = 0$ and $\dot{u}_{ix} = 0$, respectively. The calculus of φ_x and φ_y is reported in Appendix B for the sake

of clarity. We find that the potential is

$$\begin{aligned}
\varphi &= \dot{u}_{1x} \sum_{n=1}^{\infty} \phi_{1n} [\cos(n\sigma) \cosh(n(\tau - \tau_2)) - \cosh(n\tau_2)] \\
&+ \dot{u}_{1y} \sum_{n=1}^{\infty} \phi_{1n} \sin(n\sigma) \cosh(n(\tau - \tau_2)) \\
&+ \dot{u}_{2x} \sum_{n=1}^{\infty} \phi_{2n} [\cos(n\sigma) \cosh(n(\tau - \tau_1)) - \cosh(n\tau_1)] \\
&+ \dot{u}_{2y} \sum_{n=1}^{\infty} \phi_{2n} \sin(n\sigma) \cosh(n(\tau - \tau_1)) \\
&= \dot{\mathbf{u}}_1 \cdot \mathbf{h}_1 + \dot{\mathbf{u}}_2 \cdot \mathbf{h}_2,
\end{aligned} \tag{13}$$

with ϕ_{in} given by (B.4).

The calculation of the fluid pressure follows from the Bernoulli equation (5), leading to

$$p - p_\infty = -(\ddot{\mathbf{u}}_1 \cdot \mathbf{h}_1 + \ddot{\mathbf{u}}_2 \cdot \mathbf{h}_2 + p_q), \tag{14}$$

with

$$\begin{aligned}
p_q &= \dot{\mathbf{u}}_1 \cdot \frac{\partial \mathbf{h}_1}{\partial t} + \dot{\mathbf{u}}_2 \cdot \frac{\partial \mathbf{h}_2}{\partial t} + \frac{[\nabla(\dot{\mathbf{u}}_1 \cdot \mathbf{h}_1 + \dot{\mathbf{u}}_2 \cdot \mathbf{h}_2)]^2}{2}, \\
&= -(\dot{\mathbf{u}}_1 \cdot \nabla \mathbf{h}_1 + \dot{\mathbf{u}}_2 \cdot \nabla \mathbf{h}_2) \cdot \dot{\mathbf{u}}_O + \frac{[\nabla(\dot{\mathbf{u}}_1 \cdot \mathbf{h}_1 + \dot{\mathbf{u}}_2 \cdot \mathbf{h}_2)]^2}{2},
\end{aligned} \tag{15}$$

and $\dot{\mathbf{u}}_O = (\dot{\mathbf{u}}_1 + \dot{\mathbf{u}}_2)/2$. The terms $\ddot{\mathbf{u}}_i \cdot \mathbf{h}_i$ come from the time variation of the fluid potential due to the motion of the cylinders. The term p_q is quadratic in $(\dot{\mathbf{u}}_1, \dot{\mathbf{u}}_2)$ and comes from the spatial variations of the fluid potential. This variation is due to the motion of the cylinders (first right hand side term of (15)) and to the convective term of the Navier-Stokes equation (last RHS term).

The integration of (14) on $\partial\Omega_i$ yields the fluid force on \mathcal{C}_i

$$\begin{pmatrix} \mathbf{f}_1 \\ \mathbf{f}_2 \end{pmatrix} = -\pi [C_a] \begin{pmatrix} \ddot{\mathbf{u}}_1 \\ \ddot{\mathbf{u}}_2 \end{pmatrix} + \begin{pmatrix} \mathbf{f}_{1q} \\ \mathbf{f}_{2q} \end{pmatrix}, \tag{16}$$

with $[C_a]$ the added mass matrix

$$[C_a] = \begin{pmatrix} m_{11} & 0 & m_{12} & 0 \\ 0 & m_{11} & 0 & -m_{12} \\ m_{12} & 0 & m_{11} & 0 \\ 0 & -m_{12} & 0 & m_{11} \end{pmatrix}, \quad (17a)$$

$$m_{11} = \sum_{n=1}^{\infty} \frac{4na^2 e^{-2n\tau_2}}{\tanh[n(\tau_2 - \tau_1)]}, \quad (17b)$$

$$m_{12} = \sum_{n=1}^{\infty} \frac{-4na^2 e^{-n(\tau_2 - \tau_1)}}{\sinh[n(\tau_2 - \tau_1)]}. \quad (17c)$$

These are new analytical expressions for the self and cross-added mass terms m_{11} and m_{12} . The self-added mass m_{11} relates the fluid force on \mathcal{C}_i to its own acceleration. The cross-added mass m_{12} relates the fluid force on \mathcal{C}_i to the acceleration of \mathcal{C}_j , $j \neq i$. These new expressions have the advantage to make explicit the effect of the confinement on the added mass terms: m_{11} and m_{12} depend on a and τ_i , which are functions of the separation distance, according to (7).

The terms \mathbf{f}_{iq} are quadratic in $(\dot{\mathbf{u}}_1, \dot{\mathbf{u}}_2)$ and come from the integration of p_q on $\partial\Omega_i$

$$\mathbf{f}_{iq} = \int_0^{2\pi} p_q(\sigma, \tau_i) \mathbf{n}_i \kappa_{\sigma\tau_i} d\sigma. \quad (18)$$

These quadratic terms (computed numerically) represent the part of the fluid force due to the spatial variations of the fluid potential.

Finally, note that if the cylinders are subject to an incident unsteady flow $\mathbf{v}_\infty(t)$, the fluid potential modifies to

$$\varphi = \mathbf{v}_\infty \cdot \mathbf{OM} + (\dot{\mathbf{u}}_1 - \mathbf{v}_\infty) \cdot \mathbf{h}_1 + (\dot{\mathbf{u}}_2 - \mathbf{v}_\infty) \cdot \mathbf{h}_2, \quad (19)$$

where \mathbf{OM} is the position vector of the fluid particle P . The first right hand side term ensures that $\nabla\varphi \rightarrow \mathbf{v}_\infty$ far from the cylinders. The other terms follow from (13) where $\dot{\mathbf{u}}_i - \mathbf{v}_\infty$ is the velocity of \mathcal{C}_i in the reference frame attached to the incident flow. Noting $[I]$ the identity matrix, it comes that the fluid force is

$$\begin{pmatrix} \mathbf{f}_1 \\ \mathbf{f}_2 \end{pmatrix} = \pi ([C_a] + [I]) \begin{pmatrix} \dot{\mathbf{v}}_\infty \\ \dot{\mathbf{v}}_\infty \end{pmatrix} - \pi [C_a] \begin{pmatrix} \ddot{\mathbf{u}}_1 \\ \ddot{\mathbf{u}}_2 \end{pmatrix} + \begin{pmatrix} \mathbf{f}_{1q} \\ \mathbf{f}_{2q} \end{pmatrix}, \quad (20)$$

where p_q and \mathbf{f}_{iq} are given by (15)-(18) under the change $\dot{\mathbf{u}}_i \rightarrow \dot{\mathbf{u}}_i - \mathbf{v}_\infty$. The equation (20) is similar to the Morison equation [28], which gives the inline

force on a body subject to an unsteady flow. From an experimental stand point, (20) shows that $[C_a]$ can be extracted either from the force on tubes vibrating in a fluid at rest or from the force on fixed tubes subject to an unsteady fluid flow.

4 Results

4.1 Added mass

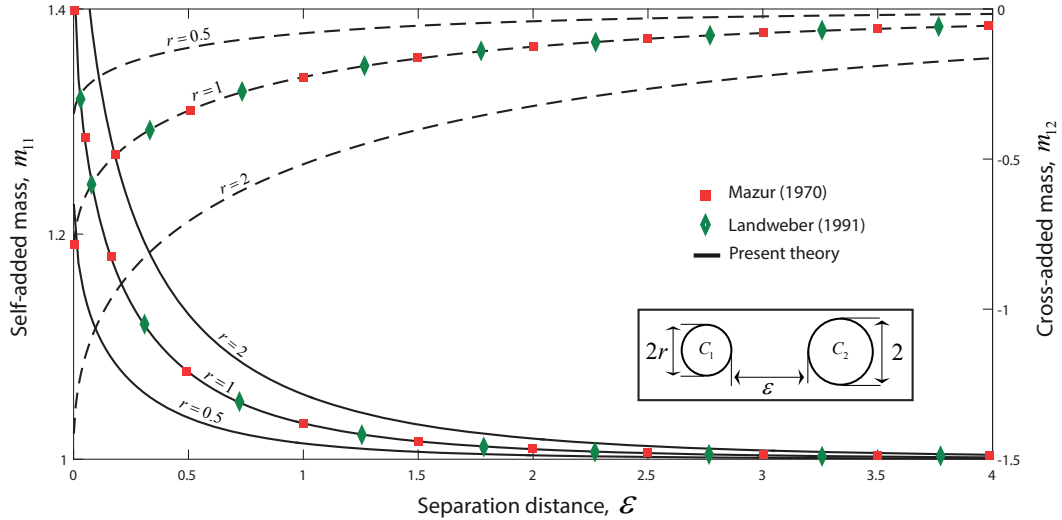


Figure 3. Self-added mass m_{11} (solid lines) and cross-added mass m_{12} , given by eq. (17), as functions of the separation distance ϵ and the radius ratio r .

In the previous section, we have obtained new simple analytical expressions for the added mass coefficients m_{11} and m_{12} . Their evolution with the separation distance ϵ and the radius ratio r is shown in Figure 3. We find that m_{11} (resp. m_{12}) decreases (resp. increases) monotonically with the dimensionless separation distance, and increases (resp. decreases) with the radius ratio. When the cylinders are in close proximity, i.e. $\epsilon \rightarrow 0$, the confinement is maximum and the added mass coefficients become unbounded, as expected. When the two cylinders are far apart, i.e. $\epsilon \rightarrow \infty$, they both behave like an isolated cylinder in an infinite fluid domain, $m_{11} \rightarrow 1$ and $m_{12} \rightarrow 0$. To validate our observations, we have reported in Figure 3 the predictions of the literature [21, 29], for $r = 1$. Unlike the current method, [29] used a conformal mapping method to solve the potential problem and extracted the added mass coefficients from the kinetic energy of the fluid. On his side, [21] extended the method of images by [14, 30] and extracted the added mass coefficients from the fluid force

acting on the cylinders. We obtain an excellent agreement with those authors (and some others reproduced in Table 1), thereby validating our prediction for m_{11} and m_{12} .

	Present reference	Païdoussis [31]	Chen [32]	Suss [33]	Dalton et al. [34]	Gibert [20]
m_{11}	1.0319	1.0320	1.0325	1.0328	1.0313	1.0250
m_{12}	-0.2269	-0.2269	-0.2265	-0.2266	-0.2245	-0.2250

Table 1

Comparison of the added mass coefficients by the present analysis with those obtained by various other authors. The prediction by Gibert [20] is a bit off because it relies on an asymptotic expansion that is valid for large ε . The table is given for $\varepsilon = 1$ and $r = 1$.

4.2 Quadratic fluid force

4.2.1 Uniform linear motion

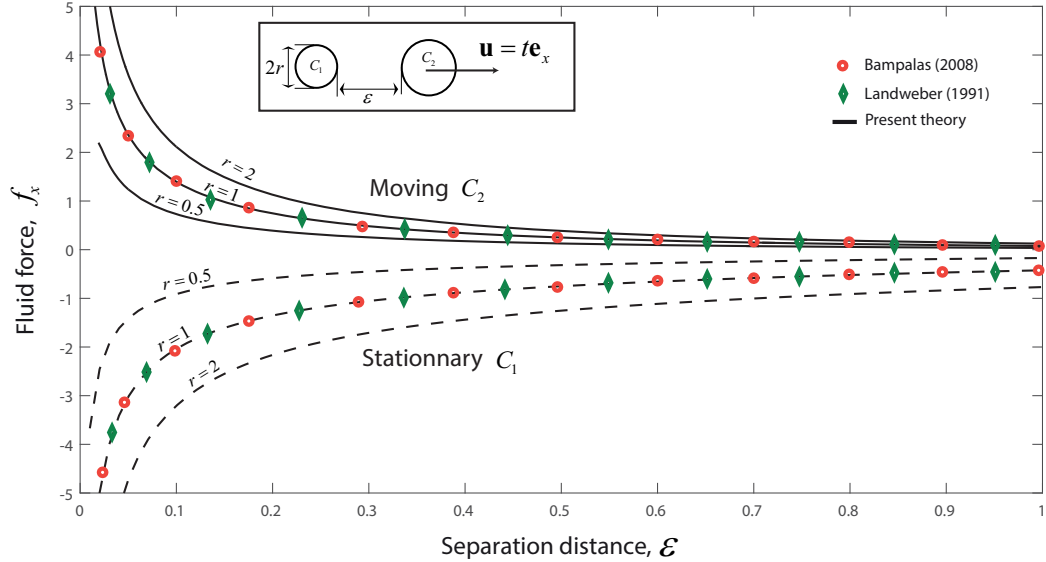


Figure 4. Fluid force, computed from eq. (16), as a function of the separation distance ε and the radius ratio r . The cylinder C_1 is stationary. The cylinder C_2 translates along the line joining the centers with a constant speed.

The fluid force is the superposition of an added mass term and a quadratic term \mathbf{f}_{iq} . In the previous section, we have validated the prediction for the added mass term and we now proceed with assessing the validity of \mathbf{f}_{iq} . To do so we consider the case in which C_1 is stationary while C_2 translates along the line joining the centers with a constant characteristic speed V_0 . The dimensionless

displacement writes $\mathbf{u} = t\mathbf{e}_x$ with $t = TV_0/R_2$ the dimensionless time. The y -component of the fluid force is $f_{iy} = 0$ by symmetry.

In Figure 4, we plot f_{ix} , given by eq. (16), as a function of the separation distance ε . We find that f_{1x} (resp. f_{2x}) is negative (resp. positive) so that the cylinders are repelled from each other. The magnitude of this repelling force decreases monotonically with ε , and increases with the radius ratio r . When the cylinders are near to contact, the force f_{ix} becomes singular and diverges to infinity. When the cylinders are far apart, the d'Alembert's paradox is at play so that no fluid force is exerted on \mathcal{C}_i . In Figure 4 the results by [35] and [21] are presented for comparison. In [35] the force is computed using a Möbius conformal mapping and a series of image singularities. Here again, we find an excellent agreement with those authors thereby validating our expression (18) for \mathbf{f}_{iq} .

4.2.2 Sinusoidal vibrations

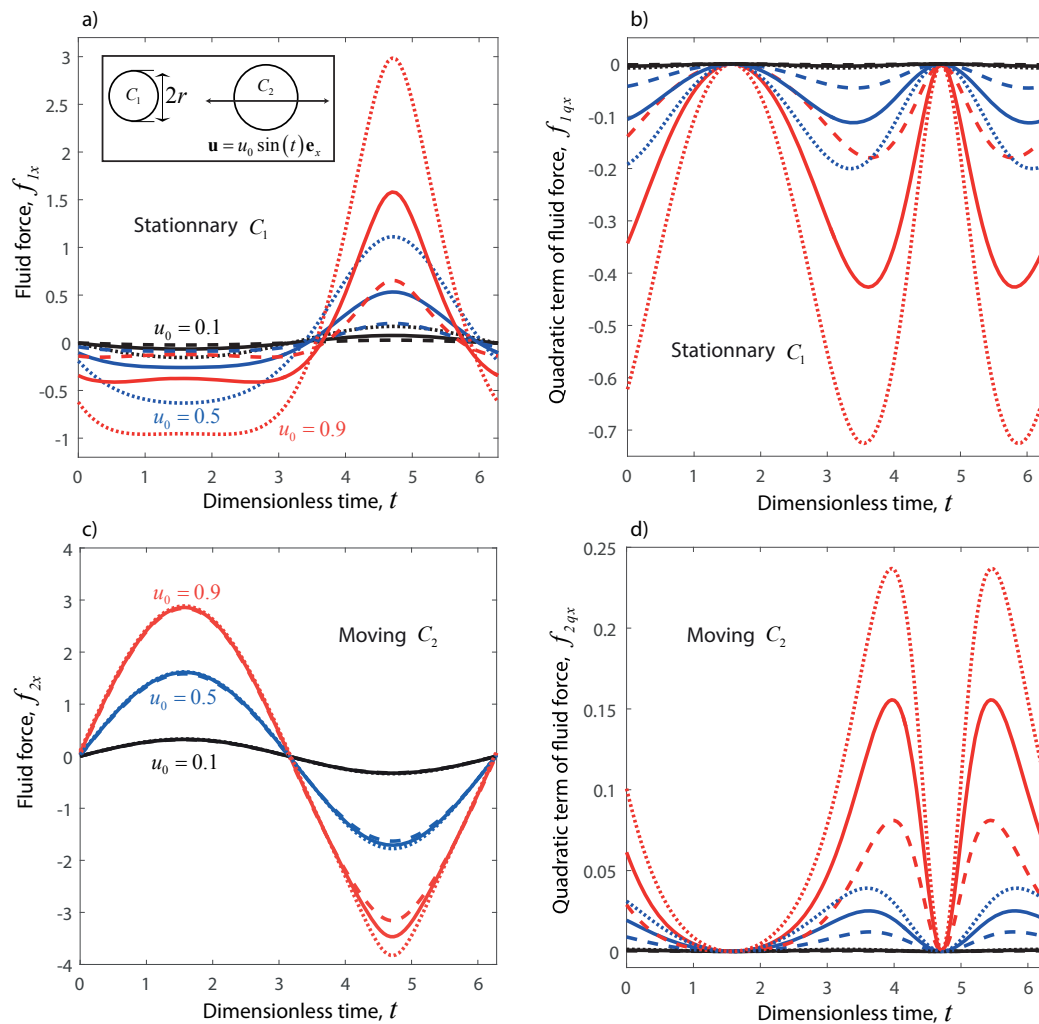


Figure 5. Fluid force, computed from eq. (16), as a function of the dimensionless time t . The cylinder C_1 is stationary. The cylinder C_2 vibrates along the line joining the centers with a dimensionless amplitude u_0 . The radius ratios are: $r = 0.5$ (dashed lines), $r = 1$ (solid lines), $r = 2$ (dotted lines). The dimensionless vibration amplitudes are $u_0 = 0.1$ (black color), $u_0 = 0.5$ (blue color) and $u_0 = 0.9$ (red color). The initial separation distance is $\varepsilon_0 = 1$. The temporal and spatial evolutions of the fluid pressure and velocity fields for $r = 0.5$ and $u_0 = 0.9$ can be observed in the corresponding movies.

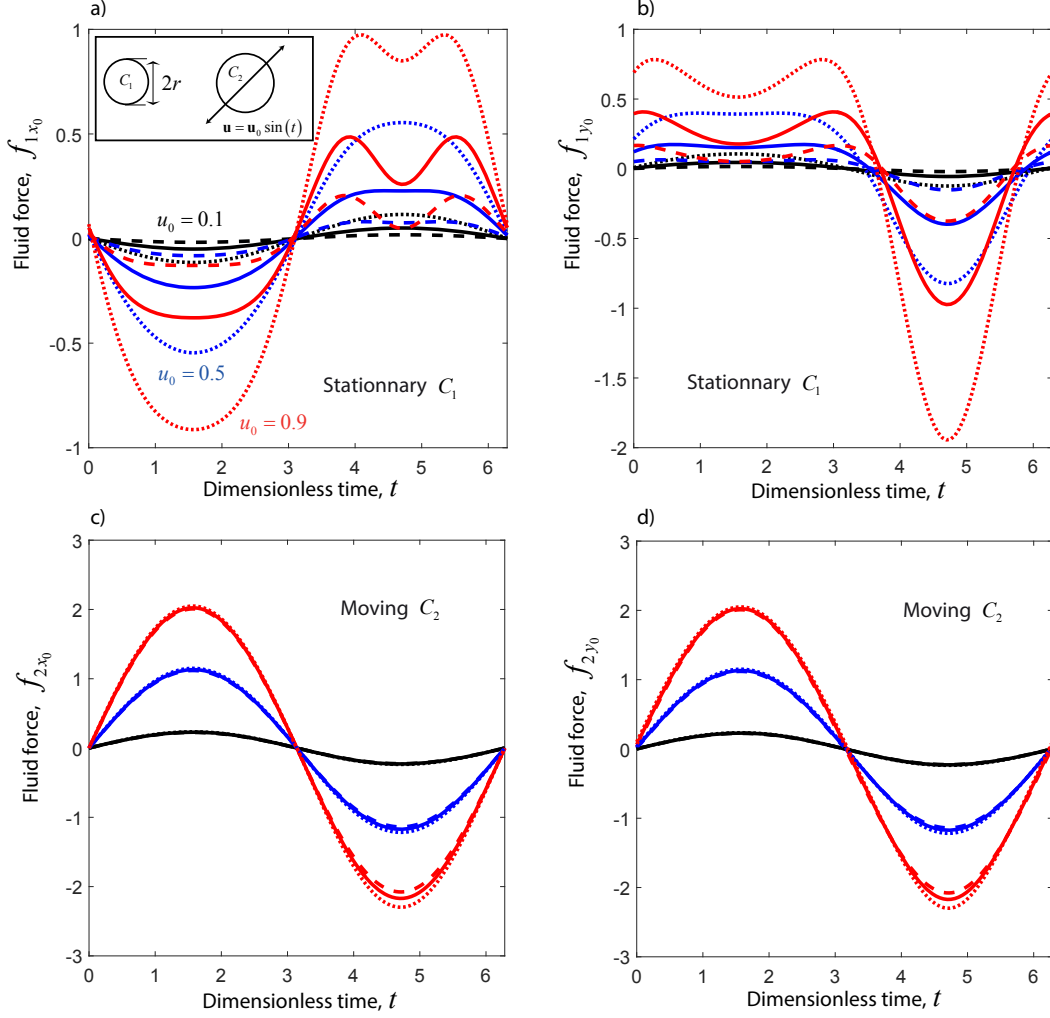


Figure 6. Fluid force, computed from eq. (16), as a function of the dimensionless time t . The cylinder C_1 is stationary. The cylinder C_2 vibrates along the direction $(\mathbf{e}_{x_0}, \mathbf{u}_0) = \pi/4$ with a dimensionless amplitude u_0 . Same legend as Figure 5.

Thus far, we have successfully compared the results of our model to those found in the literature. We now proceed with extending those results to the case in which C_1 is stationary while C_2 is imposed a sinusoidal vibration with amplitude U_0 and angular frequency Ω . We choose $V_0 = \Omega R_2$ as the characteristic speed so that the dimensionless displacement writes $\mathbf{u}(t) = u_0 \sin(t) \mathbf{u}_0$, with $\mathbf{u}_0 = \cos(\gamma) \mathbf{e}_{x_0} + \sin(\gamma) \mathbf{e}_{y_0}$. Here $\gamma = (\mathbf{e}_{x_0}, \mathbf{u}_0)$ is the angle made by the line joining the centers in the initial configuration and the direction of vibration. The initial separation distance is $\varepsilon_0 = 1$ and three vibration amplitudes are considered, $u_0 = \{0.1, 0.5, 0.9\}$. The time evolution of the fluid force is shown in Figures 5 and 6 for $\gamma = 0$ and $\gamma = \pi/4$, respectively. Note that for $\gamma = 0$ the problem is symmetric about the x -axis, such that $f_{iy} = 0$ and we only show the evolution of f_{ix} . For $\gamma = \pi/4$ the fluid force is represented through its components (f_{ix_0}, f_{iy_0}) in the initial basis $(\mathbf{e}_{x_0}, \mathbf{e}_{y_0})$.

For both cases ($\gamma = 0$, $\gamma = \pi/4$) we find that f_{1x} and u_{2x} have opposite signs, see Figures 5a) and 6a). Thus, the fluid always pushes the stationary cylinder in an axial direction that is in phase opposition with the vibration displacement. On the contrary, f_{1y} and u_{2y} have the same sign, see Figure 6b), such that the fluid pushes the stationary cylinder in a transverse direction that is in phase with the imposed displacement. We also observe that \mathbf{f}_1 has a high harmonic distortion due to the non-negligible effect of the quadratic term \mathbf{f}_{1q} , see Figure 5b). It follows that the force on the stationary cylinder is due both to the time and spatial variations of the fluid potential.

The force \mathbf{f}_2 on the moving cylinder has the same direction as the imposed displacement, see Figures 5c) and 6c-d). The quadratic term \mathbf{f}_{2q} remains negligible, see Figure 5d), such that \mathbf{f}_2 has a low harmonic distortion and approximates to $\mathbf{f}_2 = -\pi m_{11} \ddot{\mathbf{u}}_2$. Thus, the force on the moving cylinder is mainly due to the time variations of the fluid potential. Finally, we note that the magnitude $|\mathbf{f}_i|$ is maximum as the distance between the cylinders is minimum, and it increases with the radius ratio. This is of course related to a confinement effect which induces an increase of the added mass terms $|m_{11}|$ and $|m_{12}|$, as already pointed out in § 4.1.

The online movies ($r = 0.5$, $u_0 = 0.9$) show the fluid pressure distribution and its time evolution as the cylinder vibrates. As expected, a positive (resp. negative) pressure appears in the wake of the moving cylinder as it decelerates (resp. accelerates).

5 Conclusion

We have considered the problem of two moving circular cylinders immersed in an inviscid fluid. A potential theory based on a bipolar coordinate system shows that the fluid force on the cylinders is the superposition of an added mass term and a quadratic term. The added mass term comes from the time variations of the fluid potential while the quadratic term is related to its spatial variations. We provide new simple and exact analytical expressions for the fluid added mass coefficients, in which the effect of the confinement is made explicit. The self-added mass m_{11} (resp. cross-added mass m_{12}) decreases (resp. increases) with the separation distance and increases (resp. decreases) with the radius ratio. When the separation distance tends to zero, the confinement is maximum and the added mass coefficients m_{11} and m_{12} diverge to infinity. When the two cylinders are far apart, the added mass coefficients are those of a single cylinder in a fluid of infinite extent, $m_{11} \rightarrow 1$ and $m_{12} \rightarrow 0$. We then consider the case in which one cylinder is stationary while the other is translating along the line of centers with a constant speed. Our results indicate that the fluid forces are repulsive, diverge to infinity when the cylinders are in contact, and decrease to zero as they separate. These observations are

in excellent agreement with published results. Finally, we consider the case in which one cylinder is fixed while the other is imposed a sinusoidal vibration. We show that the force on the stationary cylinder and the vibration displacement have opposite axial directions but identical transverse directions. This force is strongly altered by the nonlinear effects due to the spatial variations of the fluid potential. On the other hand, the force on the vibrating cylinder is mainly due to the time variations of the potential and approximates to $\mathbf{f}_2 = -\pi m_{11} \ddot{\mathbf{u}}_2$.

Acknowledgment

The authors would like to thank Prof. C. Eloy for his valuable comments and suggestions to improve the manuscript.

A Relations between coordinates

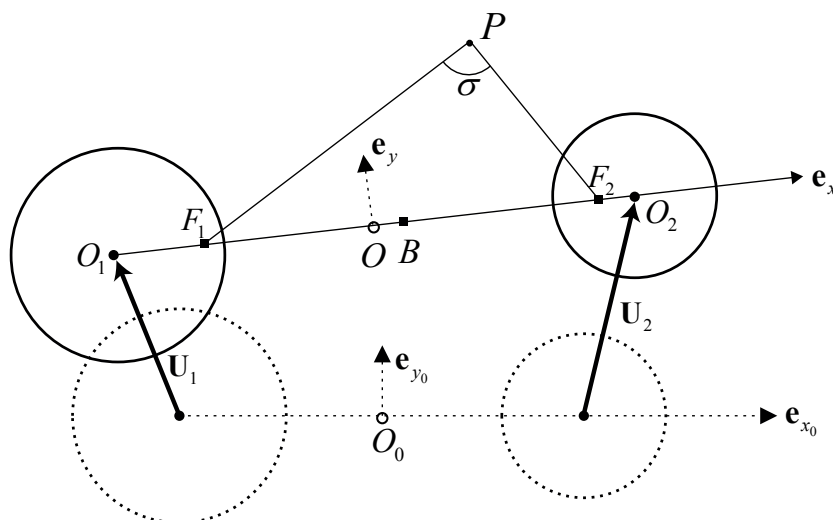


Figure A.1. Coordinate systems used for the two cylinders problem. The dashed lines represent the initial configuration whose frame of reference is $(O_o, \mathbf{e}_{x_0}, \mathbf{e}_{y_0})$. In this frame a fluid particle P has cartesian coordinates (x_0, y_0) . The solid lines represent the instantaneous configuration whose frame of reference is $(O, \mathbf{e}_x, \mathbf{e}_y)$. In this frame a fluid particle P has cartesian coordinates (x, y) and bipolar coordinates (σ, τ) .

The relations between the cartesian coordinates (x_0, y_0) (initial configuration), (x, y) (instantaneous configuration) and the bipolar coordinates (σ, τ) are, see

Figure A.1

$$\begin{pmatrix} x_0 \\ y_0 \end{pmatrix} = \frac{1}{2} \begin{pmatrix} u_{1x_0} + u_{2x_0} \\ u_{1y_0} + u_{2y_0} \end{pmatrix} + \mathbf{P} \begin{pmatrix} x \\ y \end{pmatrix}, \quad (\text{A.1})$$

$$\begin{pmatrix} x \\ y \end{pmatrix} = \begin{pmatrix} x_B + a \sinh(\tau) / (\cosh(\tau) - \cos(\sigma)) \\ a \sin(\sigma) / (\cosh(\tau) - \cos(\sigma)) \end{pmatrix} = \mathbf{g}(\sigma, \tau), \quad (\text{A.2})$$

$$\begin{pmatrix} \sigma \\ \tau \end{pmatrix} = \begin{pmatrix} \pi - 2 \tan^{-1} \left(\frac{2ay}{a^2 - (x - x_B)^2 - y^2 + \sqrt{(a^2 - (x - x_B)^2 - y^2)^2 + 4a^2 y^2}} \right) \\ \frac{1}{2} \ln \left(\frac{(x - x_B + a)^2 + y^2}{(x - x_B - a)^2 + y^2} \right) \end{pmatrix}, \quad (\text{A.3})$$

with

$$\mathbf{P} = \frac{1}{\sqrt{(d_0 + u_{2x_0} - u_{1x_0})^2 + (u_{2y_0} - u_{1y_0})^2}} \begin{pmatrix} d_0 + u_{2x_0} - u_{1x_0} & -(u_{2y_0} - u_{1y_0}) \\ u_{2y_0} - u_{1y_0} & d_0 + u_{2x_0} - u_{1x_0} \end{pmatrix}, \quad (\text{A.4})$$

the passage matrix from the basis $(\mathbf{e}_x, \mathbf{e}_y)$ to $(\mathbf{e}_{x_0}, \mathbf{e}_{y_0})$.

From (A.2) it follows that

$$y^2 + [x - (x_B + a \coth(\tau))]^2 = (a / \sinh(\tau))^2, \quad (\text{A.5})$$

so that iso- τ contours are circles of radius $a / \sinh(\tau)$ and center at $x = x_B + a \coth(\tau)$. To align $\partial \mathcal{C}_i$ with an iso-contour τ_i we thus require

$$x_B + a \coth(\tau_1) = -d/2, \quad (\text{A.6a})$$

$$a / \sinh(\tau_1) = r, \quad (\text{A.6b})$$

$$x_B + a \coth(\tau_2) = d/2, \quad (\text{A.6c})$$

$$a / \sinh(\tau_2) = 1, \quad (\text{A.6d})$$

which yields the solution (7) for x_B , a and τ_i .

The bipolar unit vectors \mathbf{e}_σ and \mathbf{e}_τ shown in Fig. 2 are expressed in the basis $(\mathbf{e}_x, \mathbf{e}_y)$ as

$$\mathbf{e}_\sigma = \frac{1}{|\partial \mathbf{g} / \partial \sigma|} \frac{\partial \mathbf{g}}{\partial \sigma} = \frac{1}{\cosh(\tau) - \cos(\sigma)} \begin{pmatrix} -\sin(\sigma) \sinh(\tau) \\ \cos(\sigma) \cosh(\tau) - 1 \end{pmatrix}, \quad (\text{A.7a})$$

$$\mathbf{e}_\tau = \frac{1}{|\partial \mathbf{g} / \partial \tau|} \frac{\partial \mathbf{g}}{\partial \tau} = \frac{1}{\cosh(\tau) - \cos(\sigma)} \begin{pmatrix} 1 - \cos(\sigma) \cosh(\tau) \\ -\sin(\sigma) \sinh(\tau) \end{pmatrix}. \quad (\text{A.7b})$$

B Determination of the fluid potential

B.0.1 Determination of φ_x

The functions φ_x and φ_y are determined with a separation of variables method with a 2π periodic function of σ , [36].

For $\dot{u}_{iy} = 0$, the fluid eqs. (11a) and (11c) are automatically satisfied by the potential function

$$\begin{aligned} \varphi_x = & \dot{u}_{1x} \sum_{n=1}^{\infty} \varphi_{1xn} [\cos(n\sigma) \cosh(n(\tau - \tau_2)) - \cosh(n\tau_2)] \\ & + \dot{u}_{2x} \sum_{n=1}^{\infty} \varphi_{2xn} [\cos(n\sigma) \cosh(n(\tau - \tau_1)) - \cosh(n\tau_1)]. \end{aligned} \quad (\text{B.1})$$

The first terms in the brackets are harmonic, 2π periodic in σ and yield a zero fluid velocity at one of the cylinder boundary. The second constant terms are added to ensure that φ_x vanishes at infinity, i.e. as $(\sigma, \tau) \rightarrow (0, 0)$.

The boundary condition (11b) yields two equations for φ_{ixn}

$$\sum_{n=1}^{\infty} \varphi_{1xn} n \cos(n\sigma) \sinh(n(\tau_1 - \tau_2)) = g_{1x}, \quad (\text{B.2a})$$

$$\sum_{n=1}^{\infty} \varphi_{2xn} n \cos(n\sigma) \sinh(n(\tau_2 - \tau_1)) = g_{2x}, \quad (\text{B.2b})$$

whose solutions are obtained by taking the scalar product

$$\langle f, h \rangle = \frac{1}{\pi} \int_0^{2\pi} f(\sigma) h(\sigma) d\sigma, \quad (\text{B.3})$$

of both sides by $\cos(n\sigma)$, leading to

$$\varphi_{1xn} = \frac{\langle \cos(n\sigma), g_{1x}(\sigma) \rangle}{n \sinh(n(\tau_1 - \tau_2))} = \frac{-2nae^{n\tau_1}}{n \sinh(n(\tau_1 - \tau_2))} = \phi_{1n}, \quad (\text{B.4a})$$

$$\varphi_{2xn} = \frac{\langle \cos(n\sigma), g_{2x}(\sigma) \rangle}{n \sinh(n(\tau_2 - \tau_1))} = \frac{-2nae^{-n\tau_2}}{n \sinh(n(\tau_2 - \tau_1))} = \phi_{2n}. \quad (\text{B.4b})$$

B.0.2 Determination of φ_y

For $\dot{u}_{ix} = 0$, the fluid eqs. (11a) and (11c) are automatically satisfied by the potential function

$$\begin{aligned} \varphi_y = & \dot{u}_{1y} \sum_{n=1}^{\infty} \varphi_{1yn} \sin(n\sigma) \cosh(n(\tau - \tau_2)) \\ & + \dot{u}_{2y} \sum_{n=1}^{\infty} \varphi_{2yn} \sin(n\sigma) \cosh(n(\tau - \tau_1)). \end{aligned} \quad (\text{B.5})$$

The boundary condition (11b) yields two equations for φ_{iyn}

$$\sum_{n=1}^{\infty} \varphi_{1yn} n \sin(n\sigma) \sinh(n(\tau_1 - \tau_2)) = g_{1y}, \quad (\text{B.6a})$$

$$\sum_{n=1}^{\infty} \varphi_{2yn} n \sin(n\sigma) \sinh(n(\tau_2 - \tau_1)) = g_{2y}, \quad (\text{B.6b})$$

whose solution are obtained by taking the dot product of both sides by $\sin(n\sigma)$

$$\varphi_{1yn} = \frac{\langle \sin(n\sigma), g_{1y}(\sigma) \rangle}{n \sinh(n(\tau_1 - \tau_2))} = \frac{-2nae^{n\tau_1}}{n \sinh(n(\tau_1 - \tau_2))} = \phi_{1n}, \quad (\text{B.7a})$$

$$\varphi_{2yn} = \frac{\langle \sin(n\sigma), g_{2y}(\sigma) \rangle}{n \sinh(n(\tau_2 - \tau_1))} = \frac{-2nae^{-n\tau_2}}{n \sinh(n(\tau_2 - \tau_1))} = \phi_{2n}. \quad (\text{B.7b})$$

References

- [1] S. B. Furber, J. E. FfowcsWilliams, Is the weis-fogh principle exploitable in turbomachinery?, *Journal of Fluid Mechanics* 94 (1979) 519–540.
- [2] S. Nair, E. Kanso, Hydrodynamically coupled rigid bodies, *Journal of Fluid Mechanics* 592 (2007) 393–411.
- [3] S. S. Chen, Vibration of nuclear fuel bundles, *Nucl. Eng. Des.* 35 (1975) 399–422.
- [4] S. S. Chen, Dynamics of heat exchanger tube banks, *J. Fluid. Eng.* 99 (1977) 462–469.
- [5] C. Le Cunff, F. Biolley, E. Fontaine, S. Etienne, M. L. Facchinetti, Vortex-induced vibrations of risers: theoretical, numerical and experimental investigation, *Oil & Gas Science and Technology* 57 (2002) 59–69.
- [6] E. De Langre, Effects of wind on plants, *Annual Review of Fluid Mechanics* 40 (2008) 141–168.
- [7] O. Doare, S. Michelin, Piezoelectric coupling in energy-harvesting fluttering flexible plates: linear stability analysis and conversion efficiency, *J. Fluids Struct.* 27 (2011) 1357–1375.

- [8] K. Singh, S. Michelin, E. De Langre, Energy harvesting from axial fluid-elastic instabilities of a cylinder, *Journal of Fluids and Structures* 30 (2012) 159 – 172.
- [9] S. Michelin, O. Doare, Energy harvesting efficiency of piezoelectric flags in axial flows, *J. Fluid Mech.* 714 (2013) 489–504.
- [10] E. Virost, X. Amandolese, P. Hemon, Coupling between a flag and a spring-mass oscillator, *Journal of Fluids and Structures* 65 (2016) 447–454.
- [11] C. Eloy, R. Lagrange, C. Souilliez, L. Schouveiler, Aeroelastic instability of cantilevered flexible plates in uniform flow, *Journal of Fluid Mechanics* 611 (2008) 97–106.
- [12] M. P. Paidoussis, S. J. Price, E. De Langre, *Fluid-structure interactions: cross-flow-induced instabilities*, Cambridge University Press, 2014.
- [13] S. S. Chen, *Flow-Induced Vibration of Circular Cylindrical Structures*, Hemisphere Publishing, 1987.
- [14] W. M. Hicks, On the motion of two cylinders in a fluid, *The Quarterly Journal of Pure and Applied Mathematics* 16 (1879) 113–140, 193–219.
- [15] H. Lamb, *Hydrodynamics*, Dover, New York, 6nd ed., 1945.
- [16] A. G. Greenhill, Functional images in cartesians, *The Quaterly Journal of Pure and Applied Mathematics* 18 (182) 356–362.
- [17] A. B. Basset, *A Treatise on Hydrodynamics*, Deighton, Bell and co., 1888.
- [18] L. H. Carpenter, On the motion of two cylinders in an ideal fluid, *J. Res. Nat. Bur. Stand.* 61 (1958) 83–87.
- [19] G. Birkhoff, *Hydrodynamics*, Princeton University Press, Princeton, New Jersey, 2nd ed., 1960.
- [20] R. J. Gibert, M. Sagner, Vibration of structures in a static fluid medium, *La Houille Blanche* 1/2 (1980) 204–262.
- [21] L. Landweber, A. Shahshahan, Added masses and forces on two bodies approaching central impact in an inviscid fluid, in: *Technical Rep. 346*, Iowa Institute of Hydraulic Research, 1991.
- [22] Q. X. Wang, Interaction of two circular cylinders in inviscid fluid, *Phys. Fluids* 16 (2004) 4412.
- [23] D. A. Burton, J. Gratus, R. W. Tucker, Hydrodynamic forces on two moving discs, *Theoret. Appl. Mech.* 31 (2004) 153–188.
- [24] A. A. Tchieu, D. Crowdy, A. Leonard, Fluid-structure interaction of two bodies in an inviscid fluid, *Phys. Fluids* 22 (2010) 107101.
- [25] Y. M. Scolan, S. Etienne, On the use of conformal mapping for the computation of hydrodynamic forces acting on bodies of arbitrary shape in viscous flow. part 2: multi-body configuration, *Journal of Engineering Mathematics* 61 (2008) 17–34.
- [26] D. G. Crowdy, Analytical solutions for uniform potential flow past multiple cylinders, *Eur. J. Mech. B/Fluids* 25 (2006) 459–470.
- [27] D. G. Crowdy, A new calculus for two-dimensional vortex dynamics, *Theor. Comput. Fluid Dyn.* 24 (2010) 9.
- [28] J. R. Morison, M. P. O Brien, J. W. Johnson, S. A. Schaaf, The force exerted by surface waves on piles, *Petroleum Transactions*, American In-

- stitute of Mining Engineers 189 (1950) 149–154.
- [29] V. Y. Mazur, Motion of two circular cylinders in an ideal fluid, *Izvestiya Akademii Nauk SSSR, Mekhanika Zhidkosti i Gaza* 6 (1970) 80–84.
 - [30] R. A. Herman, On the motion of two spheres in fluid and allied problem, *The Quarterly Journal of Pure and Applied Mathematics* 22 (1887) 204–262.
 - [31] M. P. Païdoussis, D. Mavriplis, S. J. Price, A potential-flow theory for the dynamics of cylinder arrays in cross-flow, *Journal of Fluid Mechanics* 146 (1984) 227–252.
 - [32] S. S. Chen, Crossflow-induced vibrations of heat exchanger tube banks, *Nuclear Engineering and Design* 47 (1978) 67–86.
 - [33] S. Suss, Stability of a cluster of flexible cylinders in bounded axial flow, Ph.D. thesis, McGill (1977).
 - [34] C. Dalton, R. A. Helfinstine, Potential flow past a group of circular cylinders, *Trans. ASME Journal of Basic Engineering* 93 (1971) 636–642.
 - [35] N. Bampalas, J. M. R. Graham, Flow-induced forces arising during the impact of two circular cylinders, *J. Fluid Mech.* 616 (2008) 205–234.
 - [36] R. S. Alassar, M. A. El-Gebeily, Inviscid flow past two cylinders, *ASME Trans. J. Fluid Eng.* 131 (2009) 054501.